AHMED ABDELAZIZ AMIN ALI B. ENG. (HONS) ELECTRICAL AND ELECTRONIC ENGINEERING JANUARY 2017

CHARACTERIZATION OF A MEMS-BASED HUMIDITY SENSOR

AHMED ABDELAZIZ AMIN ALI

ELECTRICAL AND ELECTRONIC ENGINEERING

UNIVERSITI TEKNOLOGI PETRONAS

JANUARY 2017

Characterization of a MEMS-Based Humidity Sensor

By

AHMED ABDELAZIZ AMIN ALI

17713

Dissertation Submitted

In Partial Fulfillment of the Requirements for the

Bachelor of Engineering (Hons)

(Electrical & Electronic Engineering)

January 2017

Universiti Teknologi PETRONAS
Bandar Seri Iskandar
31750 Tronoh
Perak Darul Ridzuan

CERTIFICATION OF APPROVAL

Characterization of a MEMS-Based Humidity Sensor

By

AHMED ABDELAZIZ AMIN ALI

17713

A project dissertation submitted to the
Electrical and Electronic Engineering Programme
Universiti Teknologi PETRONAS
in partial fulfilment of the requirement for the
BACHELOR OF ENGINEERING (Hons)
(ELECTRICAL AND ELECTRONIC ENGINEERING)

Approved by,

_____

Assoc. Prof. Dr. John Ojur Dennis

UNIVERSITI TEKNOLOGI PETRONAS
TRONOH, PERAK
January 2017

CERTIFICATION OF ORIGINALITY

This is to certify that I am responsible for the work submitted in this project, that the original work is my own except as specified in the references and acknowledgements, and that the original work contained herein have not been undertaken or done by unspecified sources or persons.

_____

Ahmed Abdelaziz Amin Ali

Abstract

Humidity sensors are very essential in many industrial processes and household appliances. They enable system operators and control mangers to fully monitor their processes in the industry. However, these sensors are miniaturized to be in micro-scale units due the development of micromachining technology. As a consequence, the sizes and the performance of the sensors have been drastically improved to be compatible with various complex systems. Whereas, the cost of the sensors have become much lower. Such devices are called Micro-Electro-Mechanical Systems (MEMS). There are many types of MEMS-Based humidity sensors such as capacitive humidity sensor and Piezoresistive humidity sensor. This research work describes the performance of a capacitive MEMS-Based humidity sensor that is fabricated using PolyMUMPS process which is a three-layer surface micromachining process. Therefore, the key purpose of this project is to mechanically and electrically characterize a MEMS-Based capacitive humidity sensor that it is actuated using electromagnetic actuation method based on Lorentz force principle. The designed integrated sensor encompasses of a sensing element and a capacitive readout circuit. To fulfill the project objectives, the available device has been mechanically and electrically characterized and its resonating plate is drop-coated by TiO_2 (Titanium Dioxide) which is a water-absorbing substance. Furthermore, a simulation of the actual device has been performed using CoventorWare software. The Theoretical values and the simulated values of the mass and the natural frequency of the resonating plate of the MEMS-Based device showed a great agreement. Consequently, an experiment has been carried to test and study the response of the humidity sensor to relative humidity throughout this research work.

Acknowledgement

First and foremost, all praise to Allah the Almighty for his blessings. I would like to express my deepest appreciation and gratitude, to my supervisor Dr. John Ojur Dennis for his guidance and expert knowledge on the subject matter and for always encouraging me to go ahead with my aspirations in both the final year project and other endeavors. I would also like to thank my co-supervisor Dr. Mohd Haris for his support during the course of my project as well as being a good friend. Special thanks to Mr. Omar my Graduate Assistant who helped in overcoming and troubleshooting any issues I faced during my simulations and experiments. My deepest gratitude to Universiti Teknologi PETRONAS (UTP) for providing the highest standards of education and guiding future generations to become the best of engineers, and to be a significant part of our societal make up.

None of my achievements in life would have been possible without the support of my family, who have always been by my side.

I would like to thank my Mother, Mona Jamaleldin, my Father, Abdelaziz Amin, my uncles, Nooreldin Amin, Abdelsalam Amin, and Saleh Eisa, as well as my grandfather Jamaleldin Mohamed, and other members of my family for the endless support and love they have given me. I never would have made it here without them. I also wish to thank my late aunt, Suzan Amin whose help has been inestimable, and I am too unfortunate that she cannot see me graduate.

Finally, it was a great experience to be a part of the UTP family, and the friends I have made as well as the moments we spent together will be cherished for many years to come.

Table of Contents

List of Figures

List of Tables

Chapter 1: Introduction

1.1 **Background**

Humidity is the presence of water vapor in air. The amount of water vapor in air disturbs human comfort and affects most of the physical, chemical, and biological processes in industries. Humidity sensing plays an integral role in most of industrial processes. The measurement of humidity in industries is very crucial as it may have an impact on the production costs as well as the health and safety of the personnel. Therefore, controlling and monitoring humidity is of utmost significance for the reliability of operation systems and the optimization of processes in domestic and industrial applications [1]. For instance, humidity sensing is required in chemical gas purification, paper and textile production, pharmaceutical and food processing, and respiratory equipment. In all of the aforementioned applications and many others, humidity sensors are used to provide an indication of the moisture levels in the environment.

There are several existing types of humidity sensors such as resistive humidity sensors, capacitive humidity sensors, thermal humidity sensors, piezoresistive humidity sensors, optical humidity sensors, and so forth [2]. Capacitive humidity sensors are extensively used amidst them because of the advantages of having low power consumption, long-range stability, and great performance [3, 4].

Due to the marvels of advanced technology in our modern era, as such sensors in micro scale units which are usually fabricated using MEMS technology are highly demanded. Micro-Electro-Mechanical Systems (MEMS) are miniaturized devices and systems which are fabricated using micromachining techniques. MEMS devices have critical physical dimensions in the range of 100 nm to 1 mm [3].

PolyMUMPs is a standard process of fabricating MEMS devices and systems. The uniqueness of the PolyMUMPs process in fabricating MEMS devices is centralized around its compatibility with many systems and ability to support different designs on a single silicon wafer [5]. Figure 1 shows an SEM image of a MEMS device that has been successfully fabricated using this latest technology was designed in UNIVERSITI TEKNOLOGI PETRONAS.

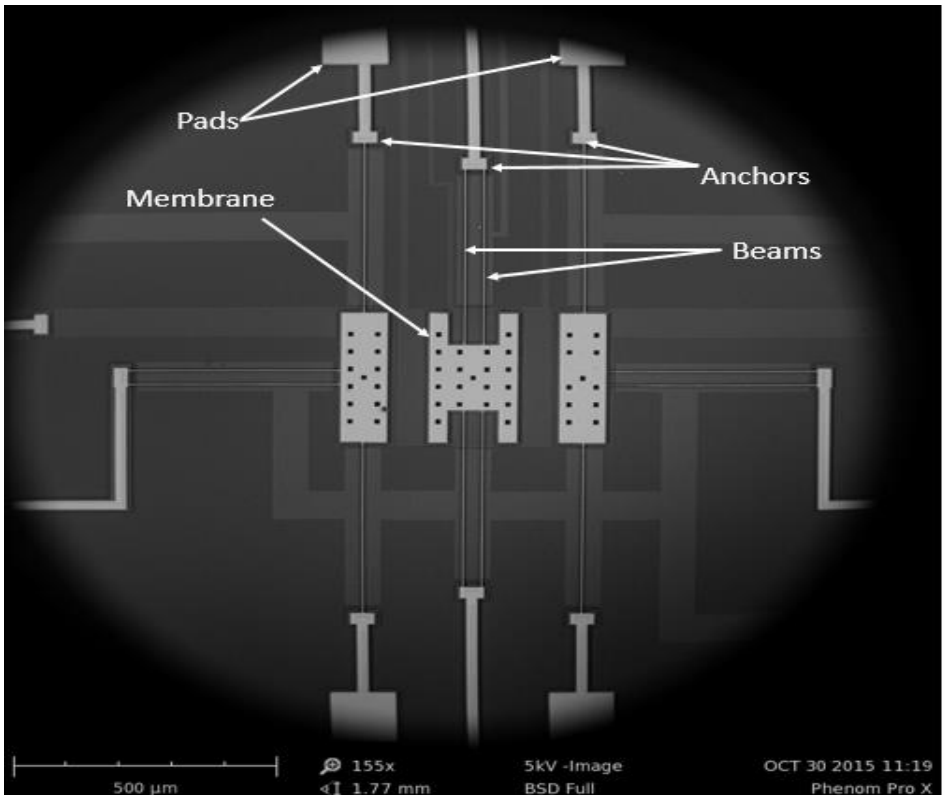

Figure 1: SEM image of the MEMS device

The PolyMUMPs process encompasses of seven physical layers and eight lithography levels. The seven physical layers include one silicon nitride layer, 2 deposited oxides layers, 3 polysilicon layers, and one metal layer [6]. The Nitride layer provides an isolation between the silicon substrate and the electrical surface layers. The polysilicon layers are used as the structural material while the metal oxide layers consist of Phosphosilicate Glass (PSG) which is used as sacrificial layers and finally the metal layer provides electrical connection to the package [5].

1.2 **Problem Statement**

Most of the humidity sensors which have been fabricated using MEMS technology are designed based on principles of capacitive, resistive, and piezoelectric elements. However, the resistive humidity sensor is susceptible to temperature hence, some error percentage in the sensor measurement is expected. Moreover, the CMOS-MEMS based piezoresistive humidity sensor has some drawbacks. These disadvantages are presented in the heater used for the electro-thermal actuation which increases the energy consumption of the device. Furthermore, the piezoresistive sensor is temperature sensitive which means that when the temperature increases, the sensitivity reduces and the resistance increases accordingly. Nevertheless, capacitive humidity sensors are not affected by changes in temperature and they have less power consumption, high sensitivity at low moisture levels, and fast response time [4]. The device is small in size (micro-scale) and it is required to investigate the effect of several factors during the operation of the humidity sensing. For example, the impact of device operating temperature and applied AC signal during experimental measurements on the humidity that affects the response of this sensor.

1.3 **Objectives and scope of study**

The general aim of this research work is to experimentally characterize the MEMS-Based humidity sensor. The specific objectives of the project are:

1) To mechanically and electrically characterize the fabricated device.
2) To test the device response to the presence of humidity in the environment.
3) To compare the experimental results with the simulation and theoretical values.

The scope of this study is to primarily characterize the device mechanically and electrically. Mechanical characterization of the device involves the calculation of its resonance frequency, mass of the resonator, spring constant, and amplitude change. While, electrical characterization covers the measurement of the output capacitance and the capacitance to voltage conversion. Secondly, the device response to humidity will be measured in testing chamber. Finally, the results obtained from the experimental work will be compared with the modeled and simulated values.

Chapter 2: Literature Review

A MEMS device has been successfully designed in UNIVERSITI TEKNOLOGI PETRONAS using three-layer polysilicon surface micromachining PolyMUMPs process. The device is designed to sense and measure relative moisture levels in the environment for various applications. The sensing principle of the PolyMUMPs device is based on capacitive sensor and it is intended to be actuated using electromagnetic method based on the Lorentz Force principle. Figure 2 shows the schematic of the top view of the fabricated MEMS humidity sensor.

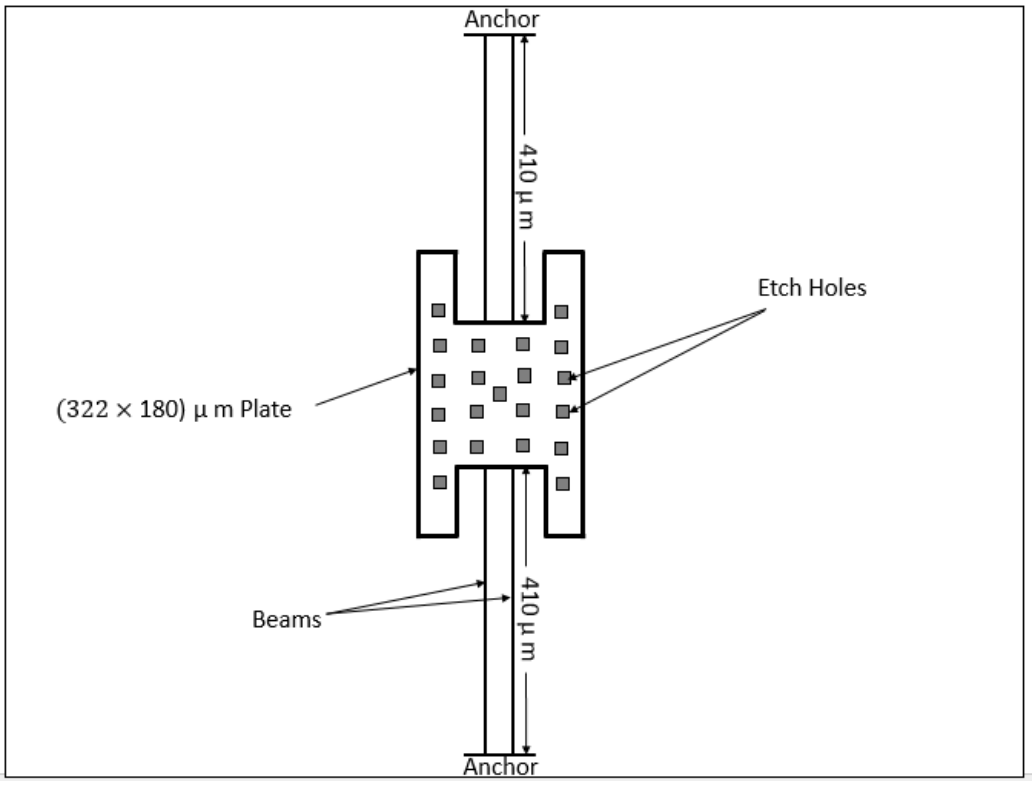

Figure 2: Schematic of the top view of the MEMS device.

The PolyMUMPs process comprises of seven consecutive layers which are Silicon Nitrate, Poly 0, Poly 1, Poly 2, 1st Oxide , 2nd Oxide, and the metal layer [5]. However, in the design of this PolyMUMPs device, poly 1 and poly 2 layers are combined together

and there is a gap of 1.5 µ m between poly 0 and the two combined layers .The schematic of the cross-section view across AA′ of the humidity sensor is illustrated in Figure 3.

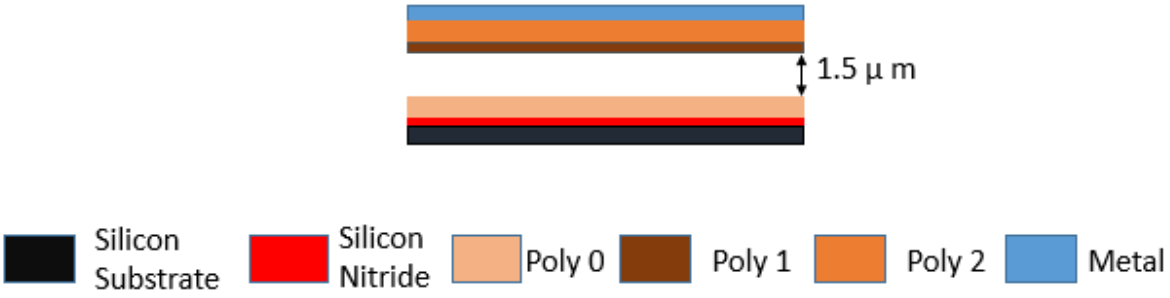

Figure 3: Schematic of the cross-section view of the MEMS device.

Figure 4 below shows the SEM image of the side view of the actual fabricated device viewing the 1.5 µ m gap between poly 0 and poly 2 layers.

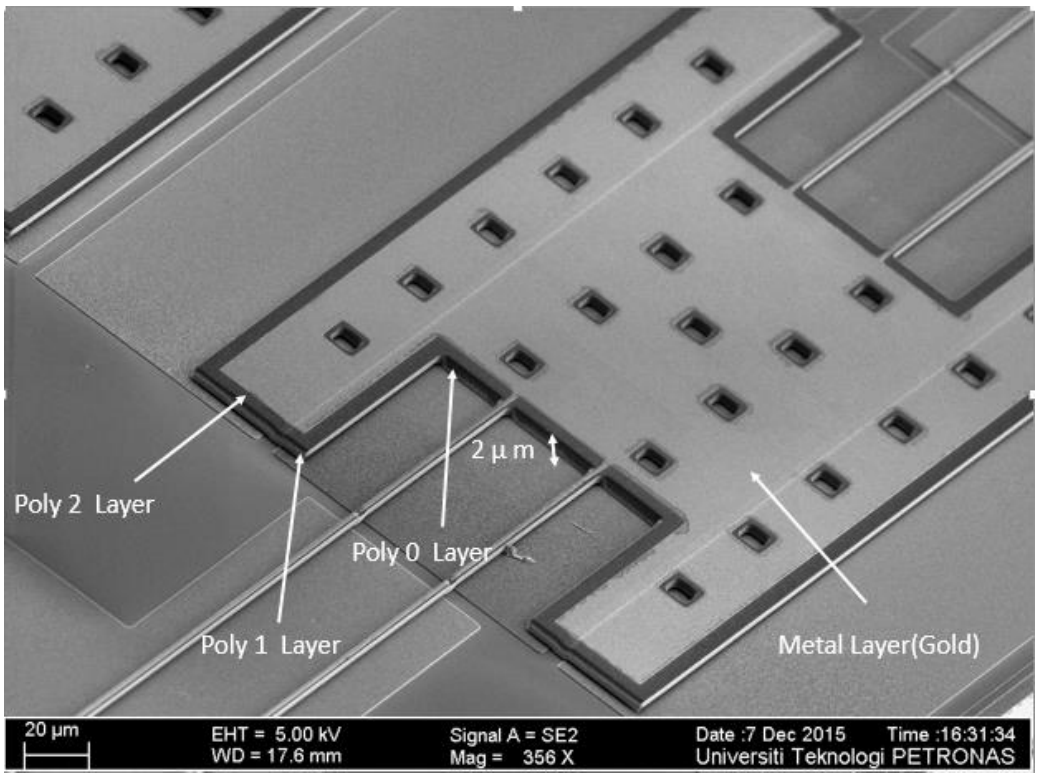

Figure 4: SEM Image of the side view of the Fabricated Device.

Electromagnetic actuators in MEMS devices produce mechanical energy on the moving plates by exploiting the electrical energy applied to the system [7]. The magnetic actuation of the PolyMUMPs device is performed by supplying an AC current through the gold metal layer on the device beams. The AC current passes through a magnetic field that is generated by placing two magnetic on the sides of the device. Consequently, a force (Lorentz Force) is generated perpendicular to the current direction and the magnetic field. The generated force is obtained by the following formula:

$$F = il \times B \tag{1}$$

Where F is the Lorentz force, i is the current carried by the wire, l is the length of the electric wire, and B is magnetic field.

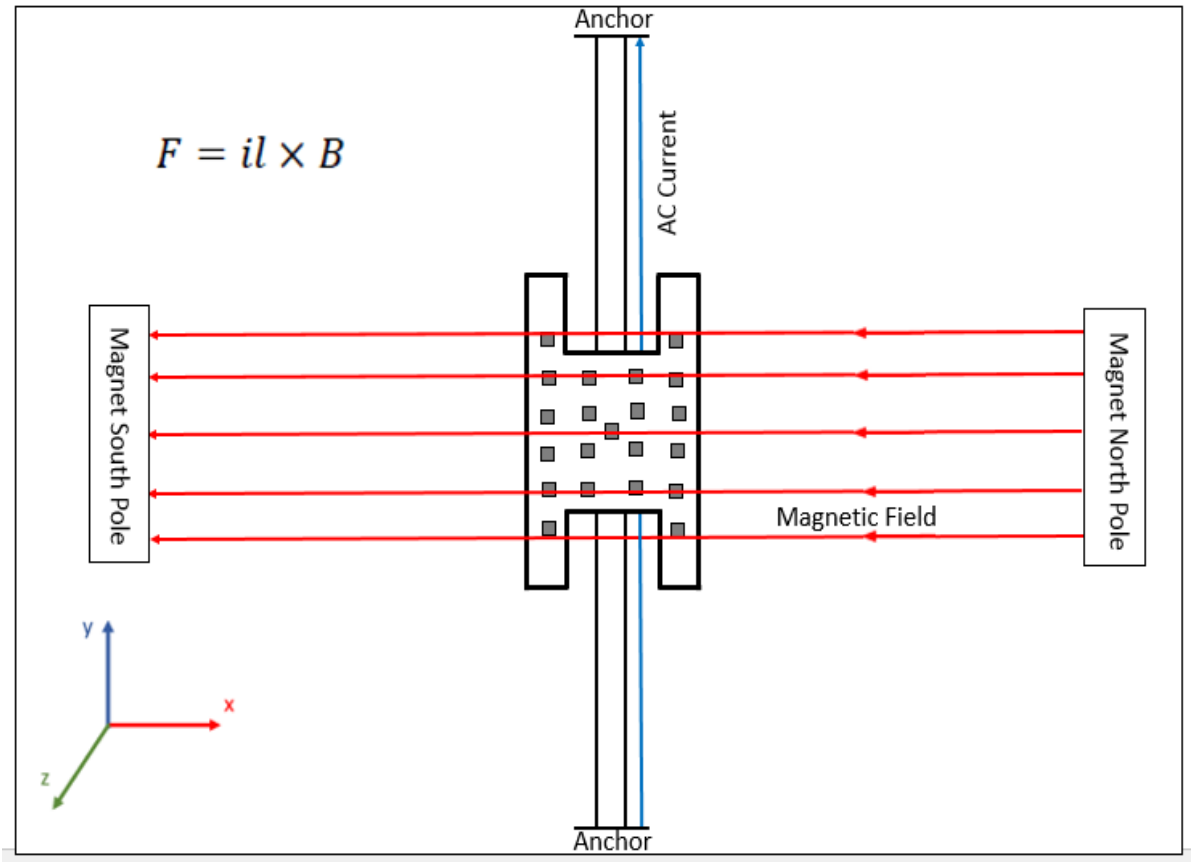

Figure 5: Schematic of Lorentz force principle

The actuation will yield a mechanical energy that generates vibration on the plate, thus the spring constant and the natural frequency are obtained for this device. The sprint constant of this device is calculated using the following formula [8]:

$$k = 4\frac{Ewt^3}{l^3} \tag{2}$$

Where E is the young's modulus, w is the width of the cantilever beam, t is the thickness of the beam, and l is the length of the beam [8].

The mass of the resonating plate is computed using the following formula [9]:

$$m = \rho \times V \tag{3}$$

Where ρ the density of the resonating is die, and V is the volume of the moving plate. Subsequently, the resonant frequency of the device is calculated as shown below:

$$f_r = \frac{1}{2\pi}\sqrt{\frac{k}{m}} \tag{4}$$

Where f_r is the resonant frequency, k is the stiffness, and m is the mass of the beams and the plate.

The humidity sensing principle of the fabricated device is based on the change mass of the resonating plate which results in changing the distance between poly 0 layer and poly 2 layer as shown in Figure 5. When the coated active layer TiO_2 (Titanium Dioxide) absorbs water molecules from the surrounding environment, the weight of the moving plate increases which decreases the distance between the two layers and the permittivity of the dielectric material increases [1, 10]. As a result, the capacitance of the coated active layer will vary accordingly. The capacitance of the sensing element on the moving plate is obtained using the following formula [9]:

$$C = \frac{\varepsilon_o \varepsilon_r A}{d} \tag{5}$$

Where *C* is the capacitance in Farads, ε_o is the permittivity of air, ε_r is the permittivity of dielectric material, *A* is the area of plate, *d* is the distance between plates in meters. The output capacitance is monitored and measured using the capacitance readout circuit IC (MS3110). The MS3110 is a chip that is responsible for sensing the change in the capacitance and providing an output voltage proportional to that change [11].

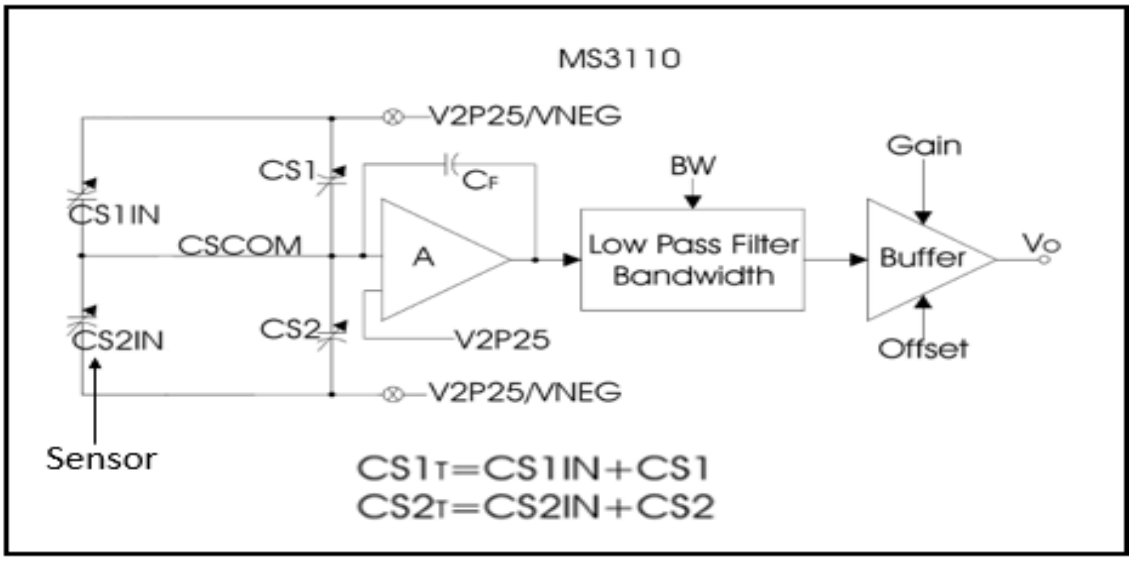

Figure 6: MS3110 Universal Capacitive Readout IC

The output voltage from the MS3110 readout circuit is calculated as follows:

$$CS2_T = CS1_{IN} + CS1 \tag{6}$$

$$CS2_T = CS2_{IN} + CS2 \tag{7}$$

$$V_O = \frac{10.26 \times (CS2_T - CS1_T)}{C_F} + V_{ref} \tag{8}$$

Where V_o is the output voltage, $(CS2_T - CS1_T)$ is the difference between the input sense capacitance, V_{ref} is the reference voltage, and C_F is designated to enhance the input sense capacitance range, $C_F \geq 1.5$pF.

Chapter 3: Methodology

3.1 **Project Flow Chart**

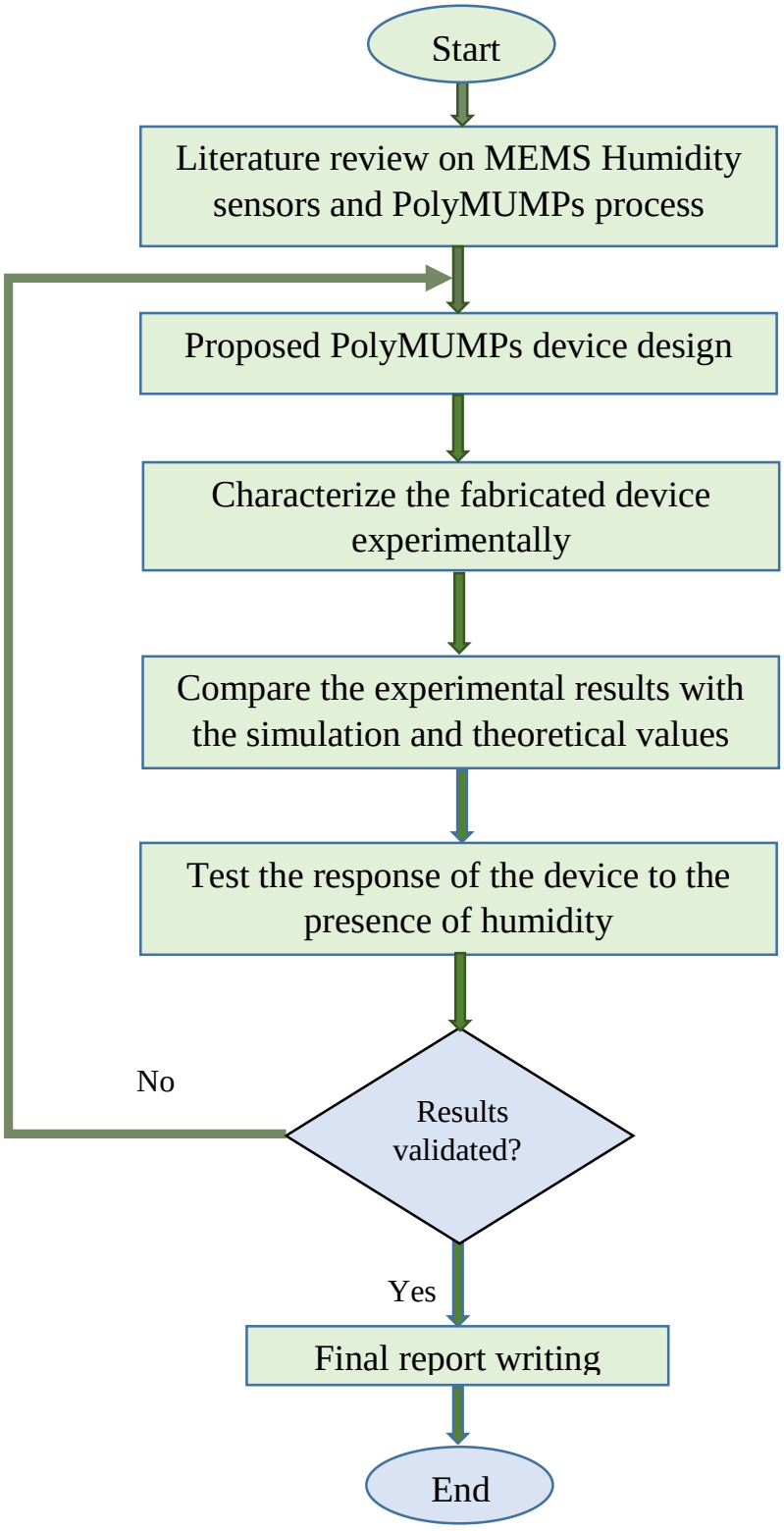

3.2 **Mathematical Modeling**

Mathematical modeling of the MEMS device is performed in order to obtain the resonance frequency and the mass for the moving plate of the device. The moving plate of this device consists of two layers which are the metal layer (Gold) and the poly 2 layer. Table 1 below shows the Young's Modulus values and the density for the moving die layers.

Layer	Young's Modulus (GPa)	Density (Kg / m^3)
Polysilicon	70	2328
Gold	78	19300

Table 1: Young's Modulus and density of the layers

The dimensions of the resonating die are presented in the following table:

Component	Width (μm)	Length (μm)	Thickness (μm)
Plate (Polysilicon layer)	180	322	3.5
Plate (Gold layer)	180	322	0.5
Beam (Polysilicon layer)	4	410	3.5
Beam (Gold layer)	2	410	0.5

Table 2: The dimensions of the resonating die

The guided beams of the device consist of two layers with different materials which are polysilicon and gold. Therefore, the average Young's Modulus is required to be calculated in order to find the spring constant of the four guided beams in equation (2). The average Young's Modulus of the beam materials is obtained by the following expression:

$$E_{ave} = \frac{E_p t_p + E_g t_g}{t_{total}} \tag{9}$$

Where E_p, t_p and are the Young's Modulus and the thickness of the polysilicon layer, while, E_g and t_g are the Young's Modulus and the thickness of the gold layer respectively [9].The expression for the mass is shown in equation (3), however, the resonator comprises of the plate and the guided-beam. Hence, the overall mass of the resonator of the device is given by [12]:

$$m = \rho_{ave} w_p l_p t_p + \frac{39}{105} \rho_{ave} w_b l_b t_b \tag{10}$$

Where w_p, l_p t_p are the plate width, length, and thickness, whereas, w_b, l_b t_b are the beam width, length, and thickness respectively, ρ_{ave} is the average density of the resonating plate which is obtained by the following formula [9]:

$$\rho_{ave} = \frac{\rho_p t_p + \rho_g t_g}{t_{total}} \tag{11}$$

Where ρ_p is the density of the polysilicon and ρ_g is the density of the gold [9]. Therefore, the resonance frequency of the resonator is obtained by substituting equations (2) and (10) in equation (4) which gives the following expression:

$$f_r = \frac{1}{2\pi} \sqrt{4 \frac{E_{ave} w t^3}{l^3 \times (\rho_{ave} w_p l_p t_p + \frac{39}{105} \rho_{ave} w_b l_b t_b)}} \tag{12}$$

3.3 **Device Simulation**

The MEMS device is simulated using CoventorWare software. Figure 7 shows FEA simulation of vertical displacement at resonant frequency which is created in the designer part of the CoventorWare software.

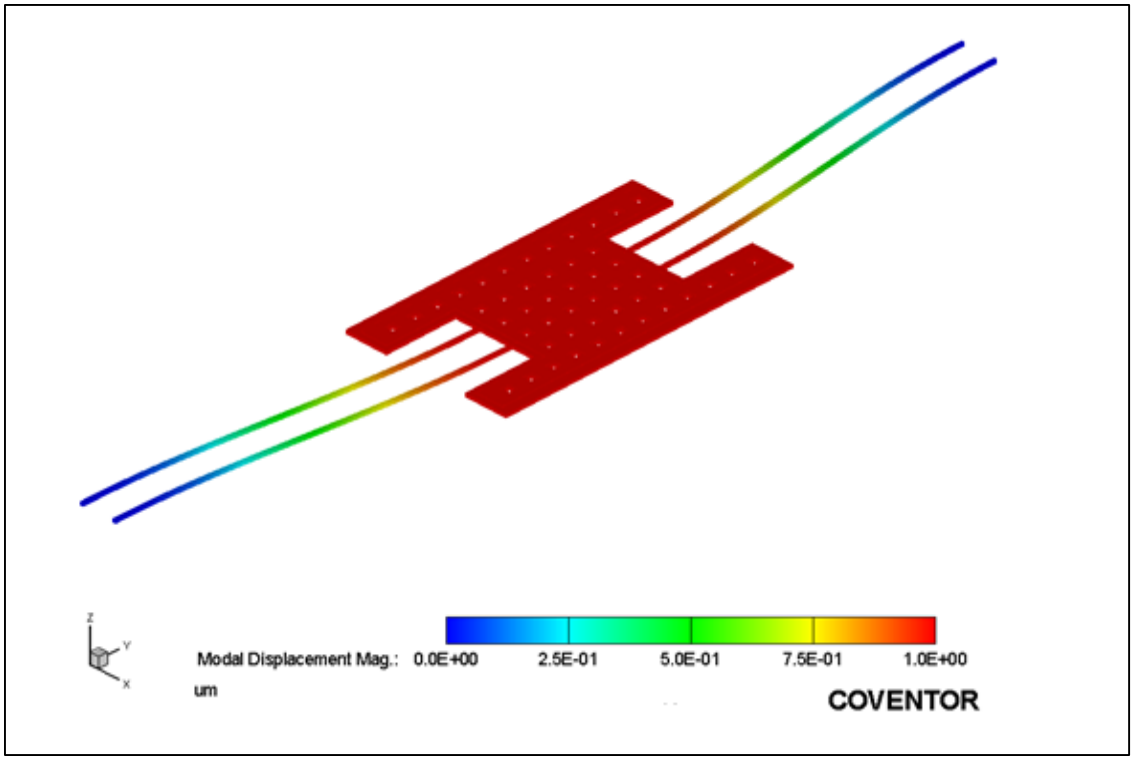

Figure 7: FEA simulation of vertical displacement at a resonant frequency of 5.13 KHz

The next step in the simulation process is to mesh the resonator of the MEMS device. As a consequence, the geometry of the structure will be reduced to a group of simpler finite elements so that precise simulation results can be achieved. The simulation results indicate a maximum displacement of approximately 1 μ m at the center of the resonator.

3.4 **Experimentation setup of the device**

The PolyMUMPs die was glued to a Printed Circuit Board (PCB) in order to connect the desired device to the laboratory equipment for testing as shown in Figure 8 below:

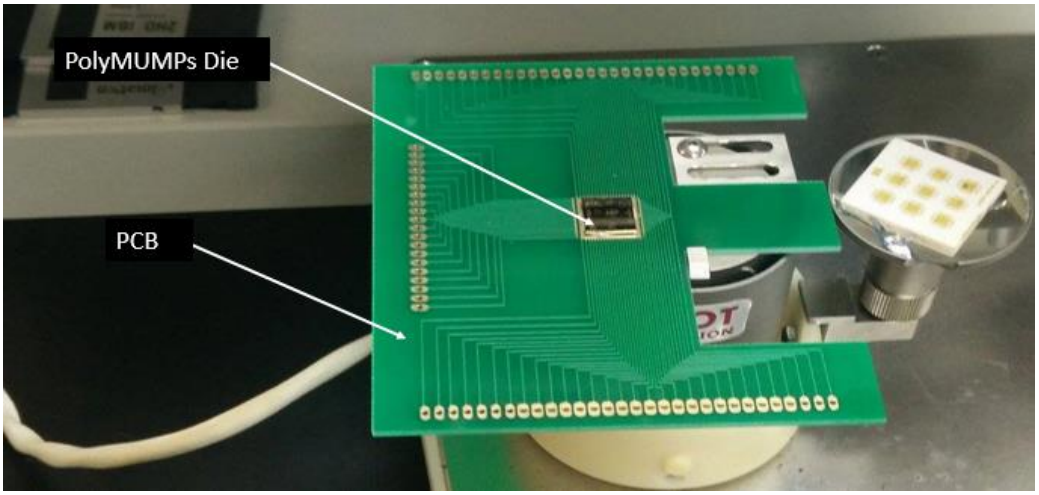

Figure 8: PolyMUMPs Die glued to a PCB

3.4.1 Drop-coating of Titanium Dioxide (TiO_2)

TiO_2 is used as humidity-sensing film which is coated on the metal layer of the moving plate of the device to absorb water molecules from the atmosphere. TiO_2 is manually drop-coated on the resonating plate using the device shown below:

Figure 9: Leica Microscope and coater

3.4.2 Device Wire-Bonding

The pads of the moving plate were manually wire-bonded by gold wires to the Printed Circuit Board using the device shown below:

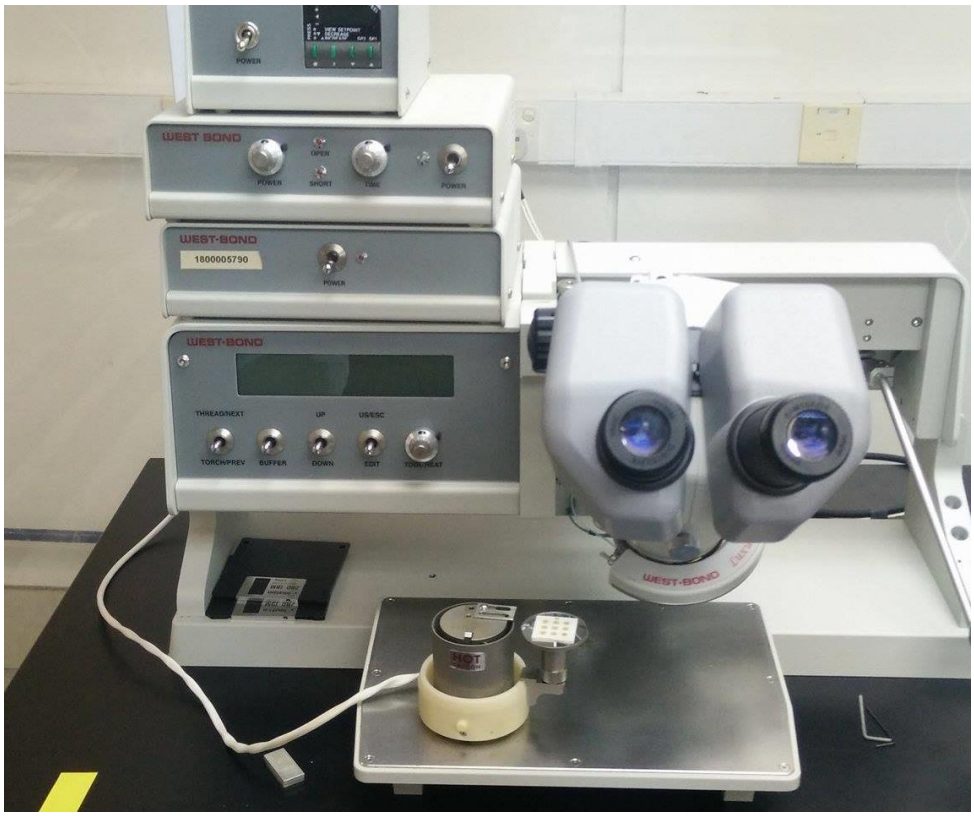

Figure 10: Leica Wire-Bonder

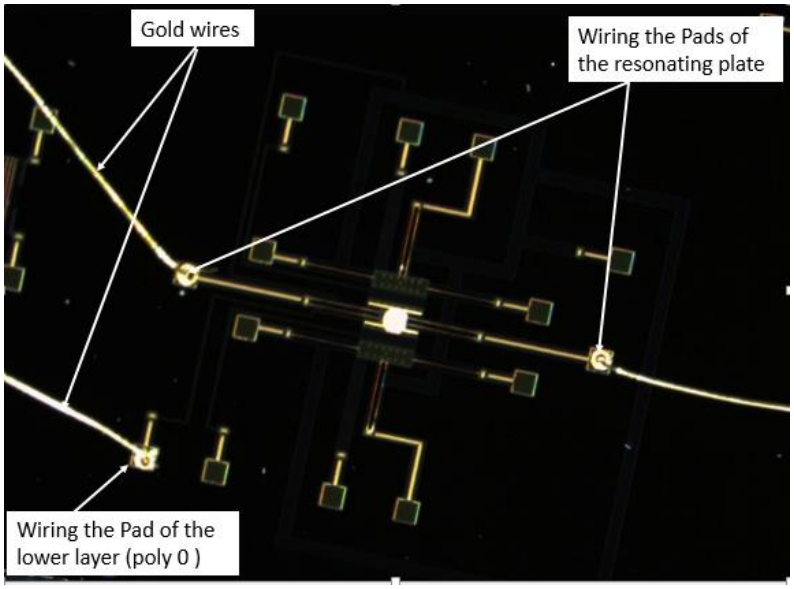

Figure 11: Wiring the pads of the device

3.4.3 Connectivity Test and Resistance Measurement

After wire-bonding the device using the wire bonding machine shown in Figure 10 , then the connectivity of the wired pins were examined using 34410A Agilent Digital MultiMeter (DMM) and the resistance between the two ports are measured and found to be 16.62 Ohms .

Figure 12: DMM used for testing connectivity and resistance measurements

3.4.4 Testing the device response to relative humidity

The device was connected to a Universal Capacitance Readout IC MS3110 from Irvine Sensors. The readout circuit can be interfaced to a single capacitive sensor or a differential capacitor pair [11].

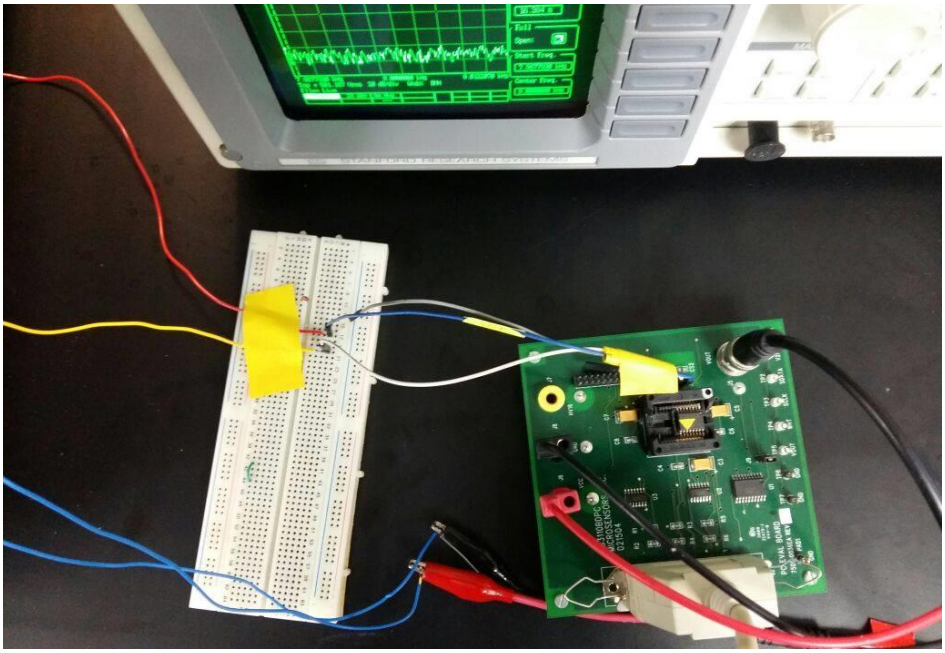

Figure 13: The connection of the IC MS3110 to the device

In this research work, it is interfaced to a single capacitive sensor by connecting the resonating plate to one end of the readout circuit and the lower layer (Poly 0) to another end of the circuit. Figure 12 shows the connection of the IC MS3110 to the device. In this part, the response of the device to relative humidity is examined using bench-top type SH-242 temperature and humidity chamber as shown in Figure 14. The dimensions of the testing chamber are $300 \times 300 \times 250$ mm. The device is put inside the chamber and then an alternate current supplied with $0.8V_{p\text{-}p}$ sinusoidal signal with a frequency of 4.5 KHz to be actuated and driven to dynamic mode. The relative humidity of the chamber is programmed to be varied from 30% RH to 90% RH with step change of 10% RH while the temperature is kept constant at $27^{\circ}C$ (room temperature). The time for each step change of 10% RH is 5 minutes and it remains constant at each step change for 3 minutes in order for the reading of the output voltage in the SR770 FFT Network Analyzer to stabilize. The time taken to measure the output voltage while changing the relative humidity and keeping the temperature constant is 66 minutes.

Figure 14: Temperature and Humidity Chamber

Figure 15 shows a permenant magent that was placed near the device in order to generate static magentic field which actuates the resonator when an input AC current is applied to the pads of the device.

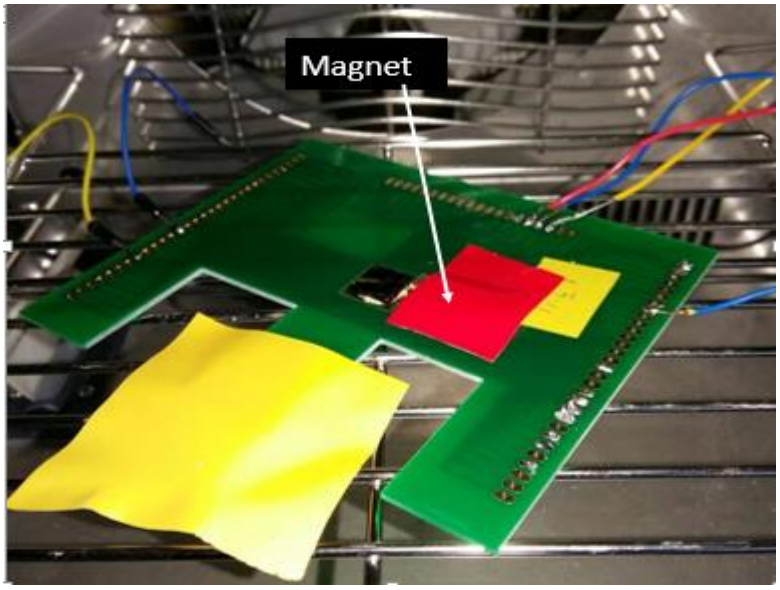

Figure 15: Permanent Magnet fixed near the Humidity sensor

The schematic drawing of the experimental setup of the device is shown in Figure 16 below:

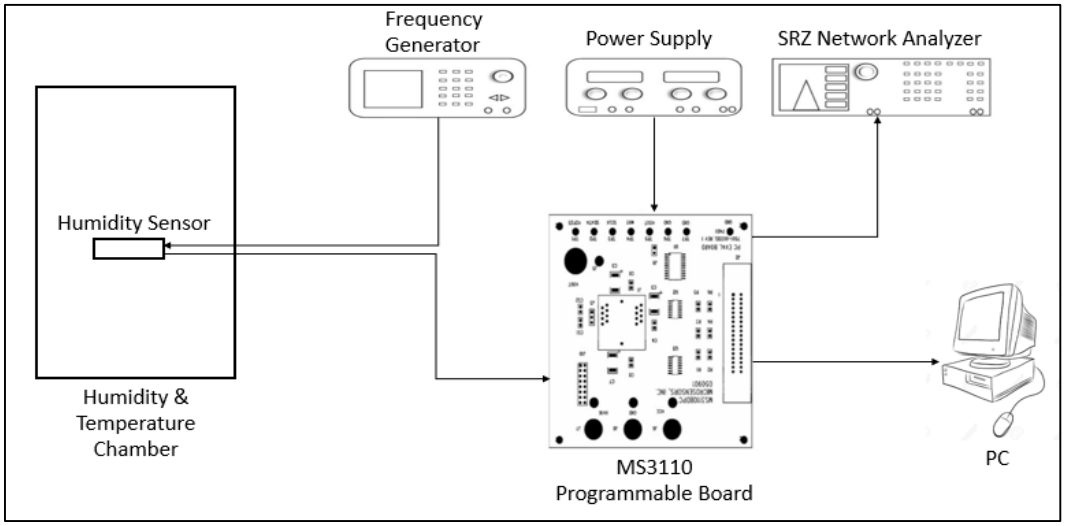

Figure 16: Schematic drawing of the experimental setup

Finally the humidity sensor was put inside the humidity chamber and then connected to other laboratory equipment as shown in Figure 17:

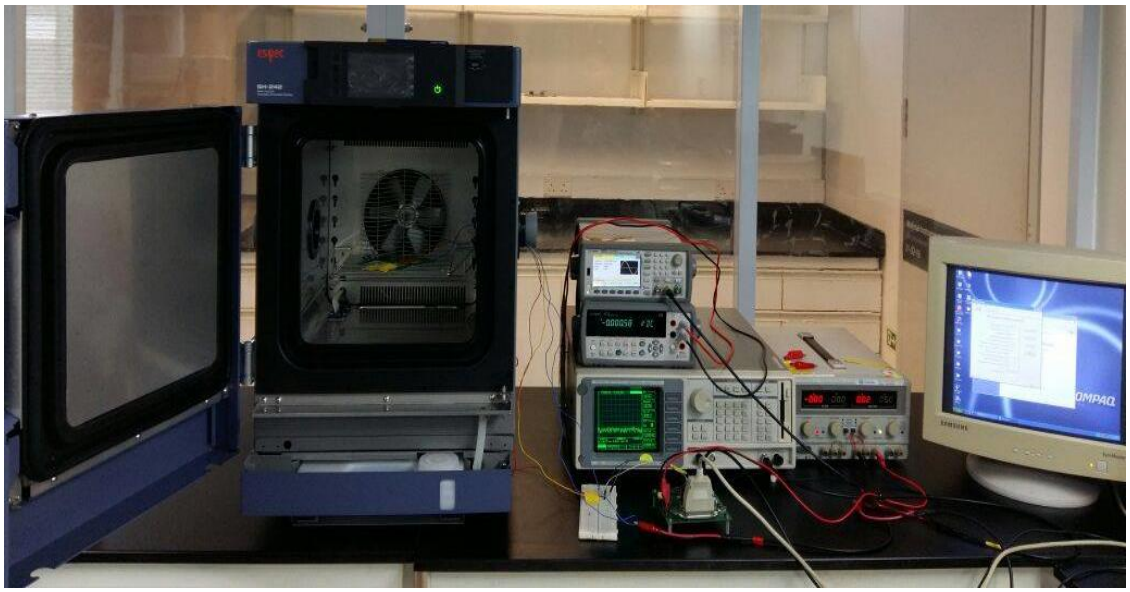

Figure 17: The connection of the humidity sensor to the laboratory equipment

3.5 **Gantt Chart**

Week / Tasks	1	2	3	4	5	6	7	8	9	10	11	12	13	14
Project Allocation														
Meetings and Discussion														
Research														
Extended Proposal														
Characterization of the fabricated device														
Proposal Defense														
Interim report submission (Draft)														
Interim report submission (Final)														

Table 3: Gantt chart of FYP I

Week / Tasks	1	2	3	4	5	6	7	8	9	10	11	12	13	14
TiO_2 Drop Coating														
Simulation of the device														
Validate the results														
Meetings and Discussion														
Progress report Submission														
Pre-SEDEX presentation														
Final report submission														
Soft bound dissertation submission														
Technical report submission														
Hard bound dissertation submission														

Table 4: Gantt chart of FYP II

Chapter 4: Results and Discussion

4.1 **Theoretical and Simulation Results**

The total Young's Modulus, the average density, and the spring constant for the resonator beams are computed to be $78\,GPa$, $6571\,kg/m^3$, and $0.67932\,N/m$, respectively. The calculated and the simulated resonance frequency and the effective mass of the resonator are illustrated in the table below:

Parameter	Symbol	Calculated Value	Simulated Value	Unit
Average Young's Modulus	E_{ave}	78	78	GPa
Average density	ρ_{ave}	6571	6571	Kg/m^3
Spring constant	k	0.67932	0.67932	N/m
Mass of the resonator	m	6.123×10^{-10}	6.237×10^{-10}	kg
Resonance frequency	f_r	5.301	5.130	KHz

Table 5: Calculated and the Simulated values of the resonator parameters

The theoretical resonant frequency of the resonator is found to be 5.301 KHz prior to the drop coating of TiO_2 (With no mass loading), while the simulated value is 5.130 KHz which yields a percent error of 3.33%. Besides, the calculated value of the resonator effective mass is 6.123×10^{-10} kg, whereas the simulated value is 6.237×10^{-10} which gives 1.8 % of error. The error of percentage in the results occurs due to some fabrication errors.

4.2 **Drop-coating of TiO_2**

The figure below shows the device after drop-coating TiO_2 on its resonator. The Titanium Dioxide coated on the resonating plate was kept for 4 days to dry under room temperature. After the TiO_2 was fully dry, the movement of the resonating plate was tested using the optical microscope to make sure that there was no damage to the shuttle during the drop-coating process.

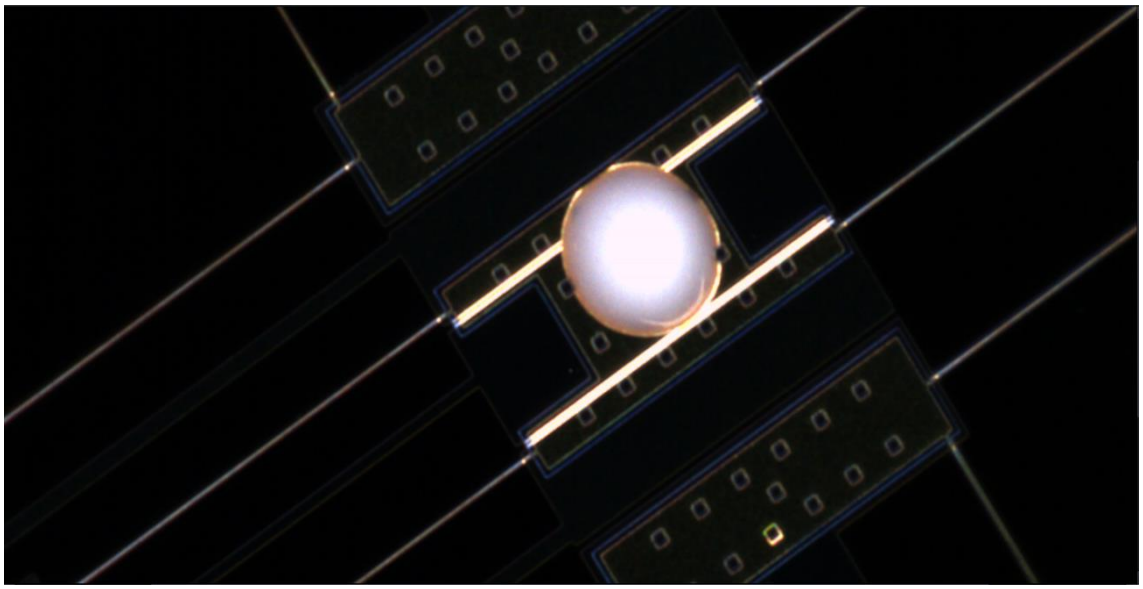

Figure 18: Drop-coating of TiO_2 on the resonator

4.3 **Experimental Results**

The experimental results obtained by testing the response of the humidity sensor to the presence of relative moisture levels in the humidity chamber. When the sensing film (TiO_2) on the moving plate absorbs water molecules in the humidity chamber, it becomes heavier and thus the distance between the moving plate and the lower plate will be varied accordingly resulting in change in the output capacitance. Nevertheless, the capacitance to voltage circuitry provides change in the output voltage in response to the change in the capacitance.

The experiment was run by applying different frequencies to the MEMS device in the testing chamber while visually observing the movement of its moving plate under the

Microscope. The plate of the MEMS started resonating at a frequency of approximately 4.5 KHz which is close enough to the resonance frequency value that was obtained from the simulation (5.13 KHz). The figures below show the plate when it is in dynamic mode under the effect of resonance frequency and when it is in static mode when the applied frequency is less than the resonance frequency of the device.

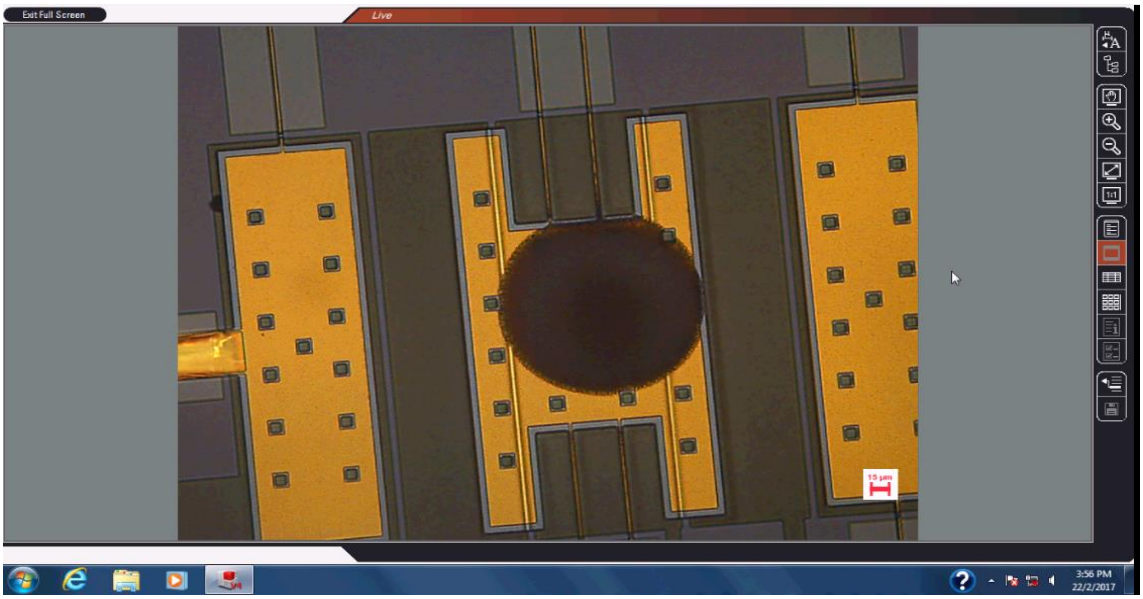

Figure 19: The plate of the device is in static mode at a frequency that is less than the resonance frequency

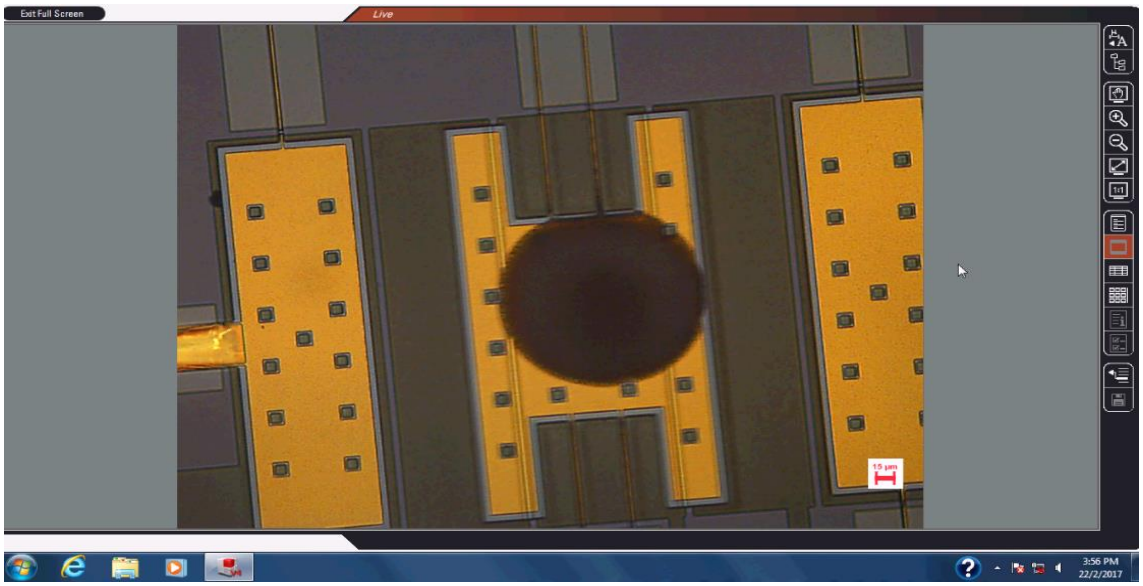

Figure 20 : The plate of the device is in dynamic mode at the resonance frequency (4.5 KHz)

Then the response of the humidity sensor to the presence of humidity has been tested inside the testing chamber for 66 minutes. An alternate current was applied with $0.8V_{p-p}$ sinusoidal signal at a frequency of 4.5 KHz to be actuated and driven to dynamic mode.

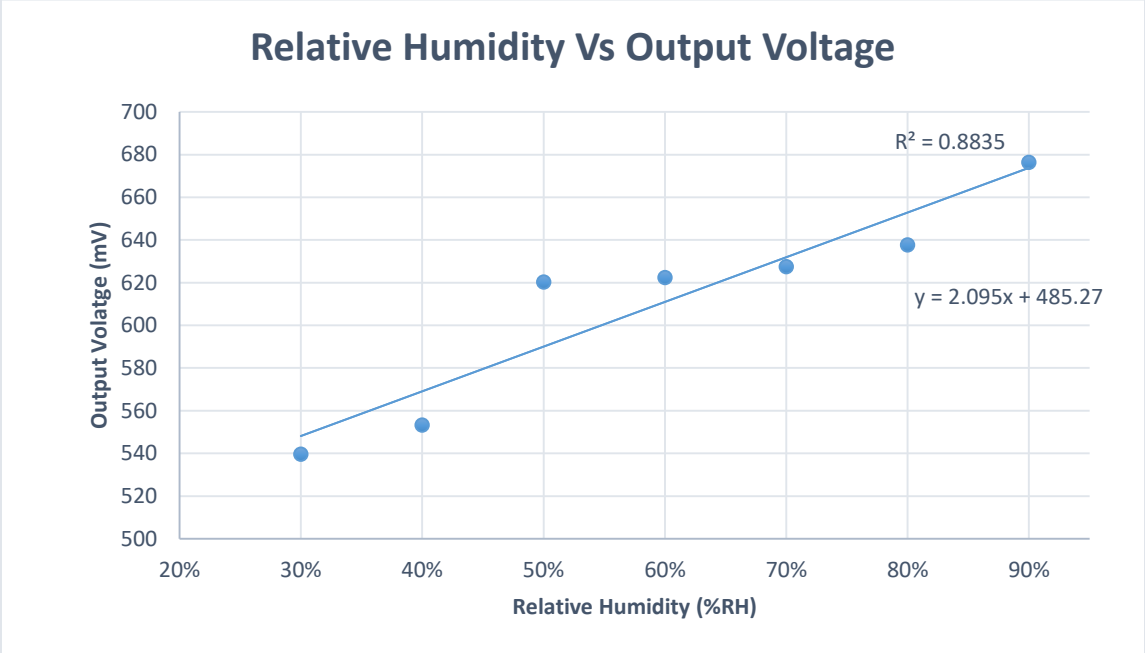

Figure 21: Relative Humidity Vs Output Voltage Graph

The graph shows a good linear correlation value of 0.8835 and a sensitivity of 2.095 mV/RH%. The output voltage is found to be 540 mV when the relative humidity in the chamber is 30% and then the relative humidity is increased with a step change of 10% while the temperature of the chamber is kept constant to 27 ºC till it reaches 90% which gives an output voltage of 676.4 mV.

Chapter 5: Conclusion and Recommendation

In conclusion, the problem statement and the objectives of this project have been clearly defined. The device has been successfully characterized mechanically and electrically . The theoretical values and the simulation values for the resonance frequency and the effective mass of the resonator were obtained. The theoretical and simulation values of the effective mass show a great agreement with a percentage difference of only 1.8%. Whereas, calculation and simulation values of the resonance frequency indicates small difference percentage of 3.33%. The response of device to the presence of the humidity in the environment has been examined and studied. The experimental value of the resonance frequency was visually observed when the device's plate started to resonate. Therefore, the resonance frequency that is actually able to drive the plate to its dynamic mode is approximately 4.5 KHz. However, the experimental resonance frequency value slightly varies from the theoretical and simulation values which are 5.301 KHz and 5.13 KHz, respectively. This slight difference in the resonance frequency values is due to some fabrication error. Subsequently, the experiment was run and the output voltage is found to be 540 mV when the relative humidity in the chamber is 30% and then the relative humidity is increased with a step change of 10% while the temperature of the chamber is kept constant to 27 ºC till it reaches 90% which gives an output voltage of 676.4 mV. The results achieved from the experiment were illustrated in a linear graph which shows that when the relative humidity increases in the testing chamber, the output voltage obtained from the Readout circuit increases accordingly. Besides, the linear graph displays great correlation and sensitivity values of 0.8835 and 2.095 mV/RH% respectively.

It is recommended to examine the response of the sensor to the change of temperature in the testing chamber. Furthermore, the effect of weather and temperature change on humidity sensing must be observed and studied. Finally, the hysteresis effect for the Relative Humidity vs Output Voltage graph must be obtained in order to confidently validate the accomplished results.

References:

[1] S. Naduvinamani and V. Mungurwadi, "Design and simulation of MEMS based humidity sensor," in *Communication and Computing (ARTCom2012), Fourth International Conference on Advances in Recent Technologies in*, 2012, pp. 164-168.

[2] J.-Q. Huang, B. Li, and W. Chen, "A CMOS MEMS Humidity Sensor Enhanced by a Capacitive Coupling Structure," *Micromachines,* vol. 7, p. 74, 2016.

[3] R. Karthick, S. Babu, A. Abirami, and S. Kalainila, "Design of High Sensitivity and Fast Response MEMS Capacitive Humidity Sensor using COMSOL Multiphysics®," *COMSOL Multiphysics MEMS Module< http://cn. comsol. com/paper/design-of-mems-based-high-sensitivity-and-fast-response-capacitive-humidity-sens-12108*.

[4] E. Terzic, J. Terzic, R. Nagarajah, and M. Alamgir, "Capacitive Sensing Technology," in *A Neural Network Approach to Fluid Quantity Measurement in Dynamic Environments*, ed: Springer, 2012, pp. 11-37.

[5] A. Cowen, B. Hardy, R. Mahadevan, and S. Wilcenski, "PolyMUMPs design handbook," *MEMSCAP Inc,* 2011.

[6] S. Wilcenski, "Introduction to Prototyping Using PolyMUMPS," *available for downloading at http://www. memscap. com/en_mumps. html*.

[7] T. Moulton and G. Ananthasuresh, "Micromechanical devices with embedded electro-thermal-compliant actuation," *Sensors and Actuators A: Physical,* vol. 90, pp. 38-48, 2001.

[8] A. Y. Ahmed, J. O. Dennis, M. H. M. Khir, and M. N. M. Saad, "Analytical modeling of mass-sensitive gas sensor based on MEMS resonator," in *National Postgraduate Conference (NPC), 2011*, 2011, pp. 1-3.

[9] M. Gafare, J. Dennis, and M. M. Khir, "Design and modeling of a CMOS-MEMS capacitive resonator based on bonded-dies for gas detection," in *Intelligent and Advanced Systems (ICIAS), 2014 5th International Conference on*, 2014, pp. 1-6.

[10] J.-O. Dennis, A.-Y. Ahmed, and M.-H. Khir, "Fabrication and characterization of a CMOS-MEMS humidity sensor," *Sensors,* vol. 15, pp. 16674-16687, 2015.

[11] "MS3110 Universal Capacitive Readout™ IC and Evaluation/Programming Manual," 2001.

[12] J. Dennis, A. Ahmed, M. M. Khir, and A. Rabih, "Modelling and Simulation of the Effect of Air Damping on the Frequency and Quality factor of a CMOS-MEMS Resonator," *Appl. Math. Infor. Sci.(AMIS),* vol. 9, pp. 729-737, 2015.

Appendix A – MS3110 Universal Capacitance Readout

MICROSENSORS
INCORPORATED

MS3110 Universal Capacitive Readout™ IC

Description:

The Universal Capacitive Readout™ IC (MS3110) is a general purpose, ultra-low noise CMOS IC intended to support a variety of MEMS sensors that require a high resolution capacitive readout interface. The MS3110 requires only a single +5VDC supply and some decoupling components. No additional components are required.

MEMS sensors (such as accelerometers, rate sensors, and other sensors that can be modeled as variable capacitors) require a readout electronic interface that can sense small changes in capacitance. The MS3110 is capable of sensing capacitance changes down to 4.0 aF/rtHz, typical.

The MS3110 interfaces to either a differential capacitor pair or a single capacitive sensor. A high-level voltage output signal that is linear with full range of sense capacitance is provided. The MS3110 also includes an on-chip capacitive DAC (up to 10pF) for initial differential adjustments and/or for quasi-differential operation with a dummy capacitor. The MS3110 has provisions for trimming the gain and output offset. Bandwidth is also user programmable. An on-chip EEPROM is provided to store trim and program settings.

Features:

- Capacitance resolution: 4.0aF/rtHz
- Sensor modes: single variable or dual differential variable
- On-chip dummy capacitor for quasi-differential operation and initial adjustment
- Gain and DC offset trim
- Programmable bandwidth adjustment 0.5 to 8kHz (9 steps)
- 2.25VDC output for ADC reference/ratiometric operation
- Single supply of +5.0VDC
- On-chip EEPROM for storage of settings
- Available in die or 16-pin SOIC

Applications:

Pressure Sensors	*Accelerometers (low g)*
Velocity Sensors	*Displacement*
Rate Sensors	*Fluid Control*
Touch Sensors	*Flow Sensors*
Motion Sensors	*Gas Sensors*

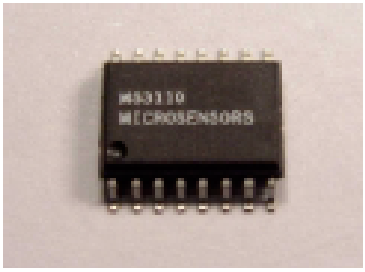

MICROSENSORS
INCORPORATED

MS3110 Universal Capacitive Readout™ IC

Functional Block Diagram:

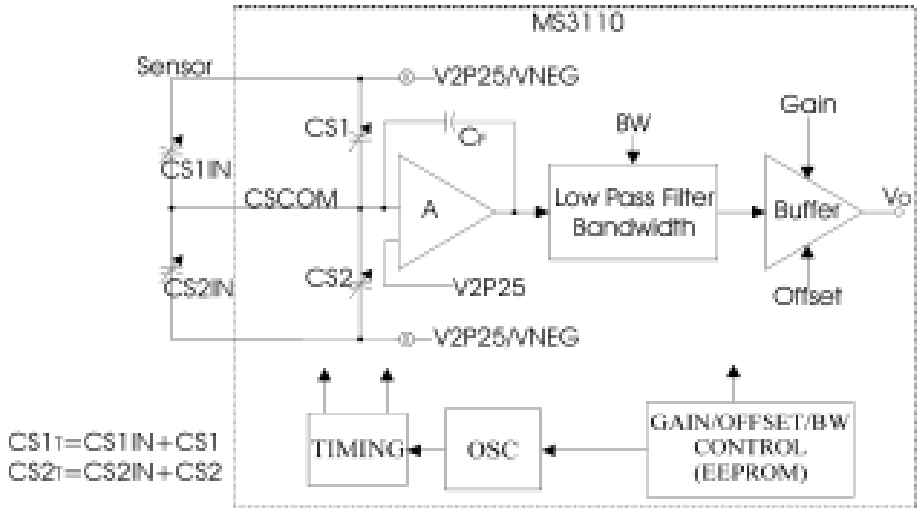

Electrical Characteristics T=25°C Unless Otherwise Spec.	Min	Typ	Max	Unit
Power Supply Voltage (+V)	4.75	5.00	5.25	V
Power Supply Current On +V		2.9	6.0	mA
Power Supply Ripple Requirement On +V			100	mV
Digital DM Inputs	- 0.5		V+	V
EEPROM Programming Voltage		16	18	V
All Other Inputs	- 0.5		V+	V
V2P25 (2.25V Reference) Trimmed	2.237		2.263	V
V2P25(2.25V Reference) Temperature Stability, Trimmed	-50		50	ppm/°C
Input Sense Capacitance($CS1_T$,$CS2_T$)	0.25		10	pF
Resolution/Input-referred Noise			4.0	aF/rtHz
CS1 Array Coarse Offset Trimmable Range, Nominal	0		9.7	pF
CS2 Array Coarse Offset Trimmable Range, Nominal	0		1.2	pF
CF Array Coarse Gain Trimmable Range, Nominal	0		19.44	pF
CF, CS1, and CS2 Trim steps	0.018	0.020	0.022	pF
Bandwidth Selection (9 steps)	500		8000	Hz
Bandwidth Tolerance	-25		+25	%
Output Voltage Range	0.5		4.0	V
Output Offset @ $CS2_T$-$CS1_T$=0, SOFF=0		2.25		V

MS3110 Universal Capacitive Readout™ IC

Electrical Characteristics	Min	Typ	Max	Unit
Output Offset @ CS1IN=CS2IN, SOFF=1		0.5		V
Output Fine Offset Trim Step		6		mV/step
Output Fine Gain Selectable Range	-15		+15	%
Output Fine Gain Trim Step		0.12		%
Output Load Resistance			10	KΩ
Output Load Capacitance		100	250	pF
Output Source and Sink Currents	2	4	7	mA
Operating Temperature Range (T_{op})	-40		+85	°C
ESD Rating			2.0	KV

THEORY OF OPERATION

The MS3110 senses the change in capacitance between two capacitors and provides an output voltage proportional to that change. The capacitors to be sensed are an external balanced pair, CS1IN and CS2IN. The output voltage is a function of the change between the sensing capacitances $CS2_T$ and $CS1_T$ according to the following:

Transfer Function: $VO = GAIN * V2P25 * 1.14 * (CS2_T-CS1_T)/CF + VREF$

Where VO is the output Voltage
Gain = 2 or 4V/V nominal
V2P25 = 2.25 VDC nominal
$CS2_T = CS2IN + CS2$
$CS1_T = CS1IN + CS1$
CF is selected to optimize for input sense capacitance range, CF ≥ 1.5pF.
VREF can be set to 0.5V or 2.25V DC for $\Delta CS = CS2_T-CS1_T = 0$. For 0.5V DC, the dynamic sensor capacity is constrained by $CS2_T$ greater or equal to $CS1_T$.

PROGRAMMING SPECIFICATIONS

To allow for such a large range of options, several program modes and trims are incorporated into the MS3110. The user has the option to store the settings into an on-chip EEPROM, which sends the data to the on-chip control registers, or program the control registers directly without memory storage. Both require serial input data, clock, and write signals. Programming the EEPROM requires a +16 VDC supply.

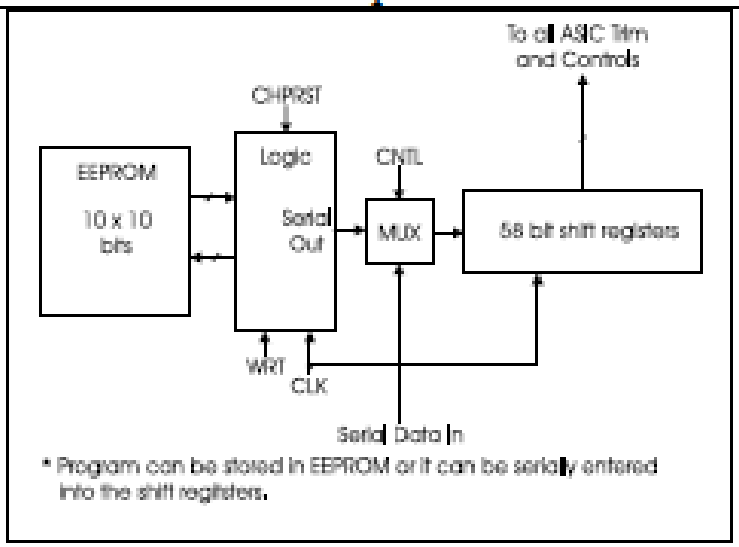

Nomenclature, definitions, and mapping into the EEPROM are provided below. Information regarding the ranges to which the bias and reference frequency should be set is also provided.

Programming Map and Modes

EEPROM Nomenclature and Description

The following programming bit descriptions and their programming map are presented below.

Nomenclature and Descriptions

Name	No. bits	Description
R[2:0]	3	Current Reference Trim Bits
T[3:0]	4	Voltage Reference Trim Bits
D[2:0]	3	Oscillator Trim Bits
B[7:0]	8	Output Buffer Gain Trim
OFF[4:0]	5	Output Buffer Offset Trim
SOFF	1	Output Buffer Output Offset Level Control
CSELCT[3:0]	4	Continuous-Time LPF Bandwidth Trim
GAINSEL	1	Output Buff Gain Selection
CF[9:0]	10	IAMP Feedback Capacitor Selection
CS1_[8:0]	9	IAMP Balance Capacitor Trim
CS2_[5:0]	6	IAMP Balance Trim Capacitor Selection

EEPROM Location Mapping:

	D9	D8	D7	D6	D5	D4	D3	D2	D1	D0
ADDR 8	R2	R1	R0	T3	T2	T1	T0	D0	D1	D2
ADDR 8		B0	B1	B2	B3	B4	B5	B6	B7	OFF0
ADDR 7	OFF1	OFF2	OFF3	OFF4	SOFF	CSELCT 3	CSELCT 2	CSELCT 1	CSELCT0	
ADDR 6		GAINSEL		CF9	CF8	CF7	CF6	CF5	CF4	CF3
ADDR 5	CF2	CF1	CF0	CS1_8	CS1_7	CS1_6	CS1_5	CS1_4	CS1_3	CS1_2
ADDR 4	CS1_1	CS1_0	CS2_0	CS2_1	CS2_2	CS2_3	CS2_4	CS2_5		
ADDR 3-0										

All other locations are unused.

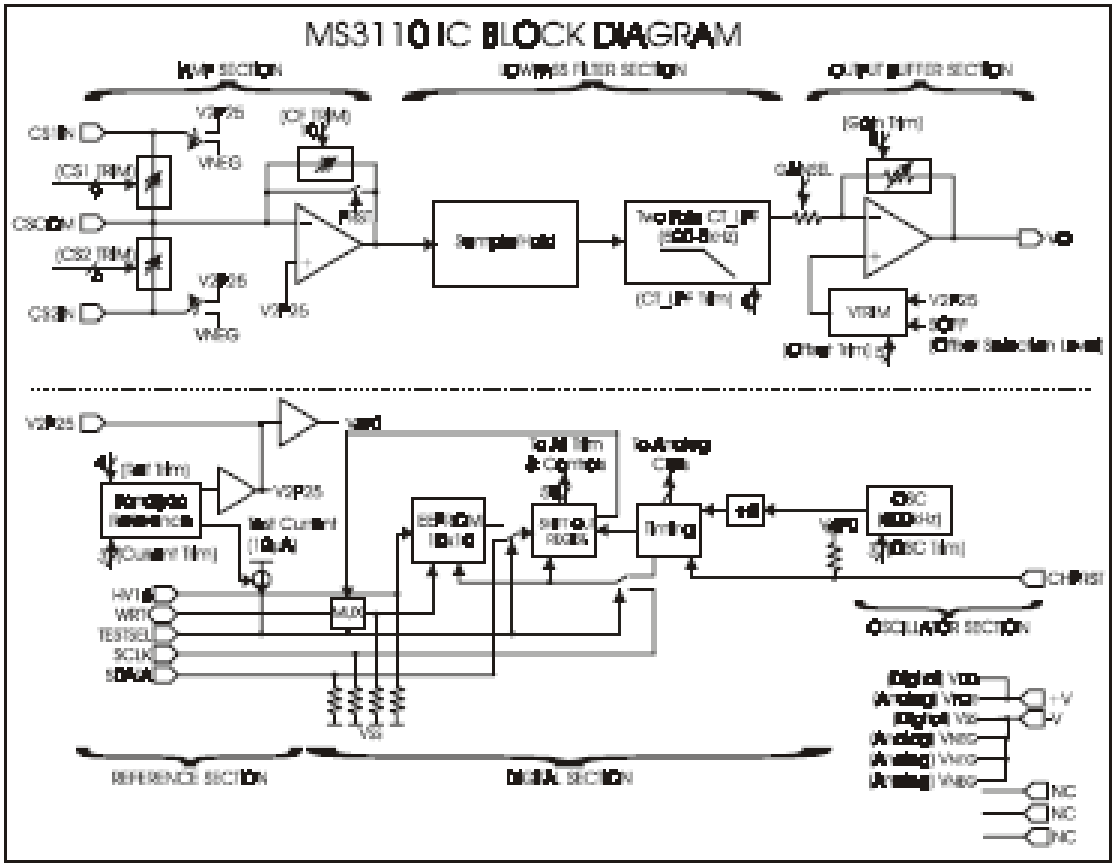

Programming Truth Tables

Bias Control Registers

Two trims are included in the master bias circuitry, bandgap trim and current reference trim. The bandgap reference voltage can be trimmed to an optimum voltage with a trim range of +/-5.1%.

Since the 2.25VDC reference tracks the bandgap reference voltage, the user can monitor the variation through pin V2P25. The reference level can be trimmed in 20 mV steps. Thus variations of the 2.25V Reference can be trimmed over process. An abridged version of the truth table is included below.

V2P25 Reference Voltage Trim (~19mV /step)

T3	T2	T1	T0	Voltage Trim
0	0	0	0	+5.1%
1	0	0	0	Nominal
1	1	1	1	-5.1%

FOR ALL APPLICATIONS, the V2P25 voltage reference should be trimmed to 2.25V +\- 10mV.

The current reference can also be monitored and trimmed. The current monitor point is brought out to the TESTSEL pin that normally selects the mode of operation for the MS3110. It also serves to monitor the internal bias current of 10µA, typical when the pin is tied to logic low. The Current reference can be trimmed in 0.8µA steps. An abridged version of the truth table is included below.

Current Reference Trim (~0.8µA/step)

R2	R1	R0	Current Trim
0	0	0	+32%
1	1	0	Nominal
1	1	1	-32%

FOR ALL APPLICATIONS, the current reference should be trimmed to 10µA +\- 2µA.

Note that if an external pull-up resistor is placed on the TESTSEL pin of the MS3110 IC, the pull-up current must be factored into the total current, or the external pull-up resistor needs to be removed before the current measurement is performed.

Oscillator Control Registers

The MS3110 has the option to trim the oscillator over process. The truth table for trim is presented below.